

Sintering Behavior of LZSA Glass-Ceramics

Oscar Rubem Klegues Montedo*, Fernando Joaquim Floriano,

Jaime de Oliveira Filho, Elídio Angoletto, Adriano Michael Bernardin

Unidade Acadêmica de Ciências, Engenharias e Tecnologia – UNACET,
Universidade do Extremo Sul Catarinense – UNESC,
P.O. Box 3167, 88806-000 Criciúma - SC, Brazil

Received: January 14, 2009; Revised: March 22, 2009

The LZSA glass-ceramic system ($\text{Li}_2\text{O-ZrO}_2\text{-SiO}_2\text{-Al}_2\text{O}_3$) shows interesting properties, such as good chemical resistance, low thermal expansion, high abrasion resistance, and a low dielectric constant. However, in order to obtain a high performance material for specific applications, the sintering behavior must be better understood so that the porosity may be reduced and other properties improved. In this context, a sintering investigation for a specific LZSA glass-ceramic system composition was carried out. A $18.8\text{Li}_2\text{O-8.3ZrO}_2\text{-64.2SiO}_2\text{-8.7Al}_2\text{O}_3$ glass was prepared by melting the solids, quenching the melt in water, and grinding the resulting solid in order to obtain a powder ($3.68\ \mu\text{m}$ average particle diameter). Subsequently, the glass powder was characterized (chemical analysis and determination of thermal properties) and the sintering behavior was investigated using optical non-contact dilatometry measurements. The results showed that the crystallization process strongly reduced the sintering in the temperature interval from 785 to $940\ ^\circ\text{C}$, and a maximum thermal shrinkage of 15.4% was obtained with operating conditions of $1020\ ^\circ\text{C}$ and 180 minutes.

Keywords: *ceramics, glass, glass-ceramics, LZSA system, sintering, crystallization*

1. Introduction

Glass-ceramics were first investigated in the 1940s by Stookey at Corning Glass¹. Since the 1940s, many systems have been extensively studied throughout the world. Because of their specific set of properties, such as good chemical and mechanical resistance, glass-ceramics have found industrial applications², military applications, and household applications such as in cooktops, cookwares and bakewares. In addition, they have been used in protection layers, sewing-thread supports in the textile industry, and ceramic tiles³. As one of the systems investigated, the LZSA ($\text{Li}_2\text{O-ZrO}_2\text{-SiO}_2\text{-Al}_2\text{O}_3$) system has shown interesting properties at low temperatures ($800\text{-}900\ ^\circ\text{C}$) and short (30-60 minutes) heat treatment times⁴. These properties include good chemical resistance and low coefficients of thermal expansion, which occur because of the very fine grain microstructure ($\sim 1\ \mu\text{m}$) of β -spodumene_{ss} (β -spodumene solid solution, $\text{Li}_2\text{O-Al}_2\text{O}_3\text{-}4\text{-}10\text{SiO}_2$) and zircon. Additionally, recent measurements of the dielectric constant (1 MHz) for laminated bodies crystallized at $850\ ^\circ\text{C}$ for 30 minutes have been carried out, and an average value of 8.61 ± 0.84 for the dielectric constant has been found⁵. Thus, applications may also be found in the electronic field. Because of these properties, several processing routes for the glass-ceramic system have been widely investigated, such as tape-casting⁵⁻⁷, extrusion⁸, and injection molding⁹. In these cases, bodies were produced through the sintering of glass powders with a high specific surface area. Montedo et al.¹⁰ evaluated the influence of the substitution of ZrSiO_4 by Al_2O_3 . Analyses of sintering behavior for the compositions studied ($6.0\ \mu\text{m}$ average particle diameter) showed that densification starts between $560\text{-}640\ ^\circ\text{C}$ and practically stops between $660\text{-}700\ ^\circ\text{C}$, resulting in the beginning of the crystallization process, i.e., densification occurred in a $90\ ^\circ\text{C}$ temperature interval. Maximum densification rates have been found to occur between 620 and $675\ ^\circ\text{C}$.

Reitz et al.¹¹ investigated the behavior of a LZSA composition made by roll-pressing using a $5.0\ \mu\text{m}$ average particle diameter powder. They found that sintering starts at $850\ ^\circ\text{C}$ and is completed at $950\ ^\circ\text{C}$. In that case, the start and finish of the densification process occur at higher temperatures due to the low density of the green bodies. Moreover, surface crystallization was observed in this glass-ceramic system⁴. In this sense, the heat treatment becomes a complex process for this glass-ceramic system because sintering and crystallization processes occur at almost the same time. According to Siligardi et al.¹², the desired order of events in a glass-powder sintering process occurs when the sintering stage comes to an end before crystallization begins, allowing for the achievement of extremely dense, low-porosity materials. This work shows the results of an investigation into the sintering behavior of a composition belonging to the LZSA glass-ceramic system, combining data obtained by differential thermal analysis (DTA), optical non-contact dilatometry analysis, X ray diffraction (XRD), and scanning electron microscopy (SEM).

2. Experimental Procedures

The composition of the LZSA glass-ceramic used in this study is shown in Table 1. The glass-ceramic was prepared with appropriate amounts of the raw materials Li_2CO_3 , ZrSiO_4 , SiO_2 , and spodumene. About 1 kg was placed in a mullite crucible and melted at $1500 \pm 3\ ^\circ\text{C}$ for 2 hours in a gas furnace. The melt was poured out into a ceramic mould so that a small glass piece could be obtained for use in measuring the thermal properties. Determination of the glass transition (T_g) and the softening point (T_s) temperatures of the small glass piece (diameter = 8 mm; length = 25 mm) was done using a dilatometer (Netzsch® DIL 402 C) in dry air at a heating rate of $5\ ^\circ\text{C}/\text{min}$. The re-

*e-mail: oscar.rkm@gmail.com

maining melt was quenched in water to obtain the frit. Then, the frit was dried and dry-crushed in porcelain ball mills for 3 hours and sieved to yield a powder. The average particle size of the glass powder was found to be 3.68 μm using a laser scattering particle size analyzer (Cilas 1064 L). Analysis of the chemical composition of the frit was carried out with X ray fluorescence spectroscopy (Phillips® PW2400). Crystallization temperatures (T_{C1} and T_{C2}) of the glass powder were determined by differential thermal analysis (DTA) in dry air at 5 °C/min in a high-temperature thermoanalyzer (Netzsch® STA 409 EP), using an empty alumina crucible as reference material. A small sample of the powder was then shaped into a cylinder using a stainless steel mould. The cylinder was used to determine the sphere and half-sphere temperatures in an optical non-contact dilatometer (Misura HSM ODHT 1400, 50 °C/min heating rate)¹³. A very small specimen (2 mm diameter and 3 mm height) was used to minimize the effects of temperature gradients inside the sample¹⁴. The method of determining the viscosity behavior was presented by Paganelli¹⁵ and is used by the optical non-contact dilatometer through the Vogel-Fulcher-Tammann (VFT) Equation:

$$\log \eta = A + \frac{B}{T - T^0} \quad (1)$$

where A, B, and T^0 are determined by solving the VFT equation with the viscosity-temperature data at the glass transition temperature, the softening point temperature, and the half-sphere temperature. Later, a powder sample was compacted by uniaxial pressing in a hydraulic press at 40 MPa (1.4 g.cm⁻³ green density) in a steel die (30 mm height and 5 mm square section). Then, the investigation of sintering behavior was carried out on the resulting green body in an optical non-contact dilatometer (Misura HSM ODHT 1400, 5 °C/min heating rate). In each thermal cycle, samples were cooled to room temperature after reaching the maximum temperature. Subsequently, each body was transversally cut, grounded and polished with 1 μm alumina paste and then etched in 2% HF for 25 seconds. All of the sintered bodies were coated with a thin Au film for analysis with scanning electron microscopy (SEM) (Philips® XL 30).

3. Results and Discussion

The composition of the glass-ceramic investigated in this work is shown in Table 1, while Figure 1 shows the amorphous nature of the glass. After considering previous work⁴, we chose this composition because of its good chemical resistance, useful thermal properties and the crystalline phases formed. A powder with a high specific surface area (3.68 μm average particle diameter) is shown in Figure 2.

Table 1. Composition (wt. (%)) of the LZSA glass-ceramic investigated.

Oxides	Composition (wt. (%))SiO ₂
SiO ₂	59.39
Al ₂ O ₃	13.57
ZrO ₂	15.61
Li ₂ O	8.64
K ₂ O	0.31
Na ₂ O	0.70
TiO ₂	0.09
Fe ₂ O ₃	0.22
CaO	0.62
P ₂ O ₅	0.82

Table 2 shows some interesting thermal properties of the glass. The glass transition temperature was found to be 598 °C. From a practical point of view, this temperature represents the beginning of the sintering process in a glass, and it is in good agreement with the one predicted by the viscosity behavior of the glass (Figure 3). It is known that the main mechanism of mass transport during sintering of vitreous materials is viscous flow¹⁶. However, according to Shyu and Lee¹⁷, this effect would be limited by the crystallization on the surface of the glass particles, since a quick increase of viscosity would take place during growth, inhibiting the viscous flow contribution to the sintering process. In fact, powders used in this work crystallized superficially because of the high specific surface area of the glass. Moreover, according to Zanotto¹⁸ and James and Jones¹⁹, the mechanism of crystallization in glasses is volumetric when the

Table 2. Thermal properties of investigated composition.

Properties	Temperatures (°C)
Glass transition temperature (T_g)	598
First crystallization temperature (T_{C1})	810
Softening point (T_s)	840
Second crystallization temperature (T_{C2})	915
Melting point (T_m)	1213
ΔT ($T_c - T_g$)	215
T_g/T_m	0.59

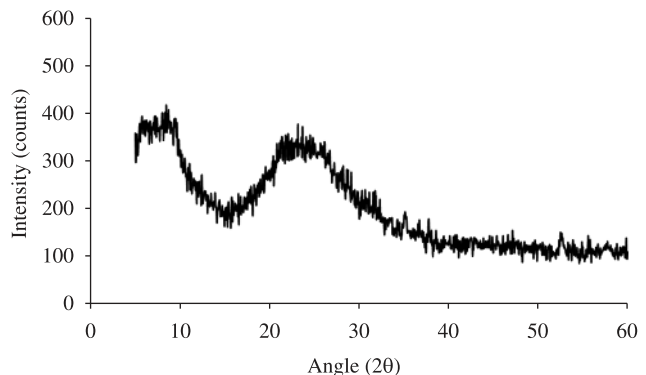


Figure 1. X ray diffraction patterns for the glass at room temperature.

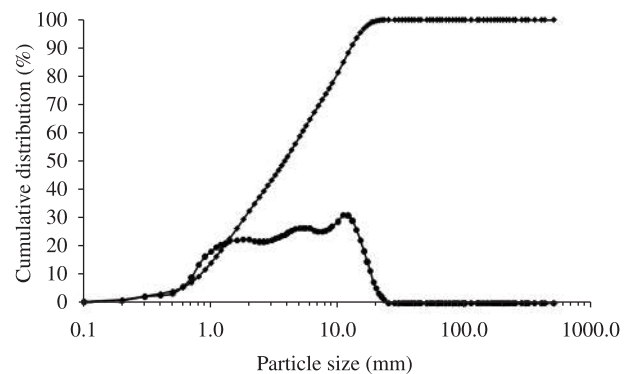


Figure 2. Powder particle size distribution of the glass.

T_g/T_m ratio is smaller than 0.58 and superficial or mixed when the ratio is higher than 0.58. So, in analyzing the T_g/T_m relation shown in Table 2 and looking at previous work⁴, we found that the composition we investigated crystallizes superficially.

This means that the viscosity increase on the surface of the particle should inhibit the sintering process and thus cause a reduction of the densification rate. Because of this, it is important to have a very large temperature interval for sintering⁴, ΔT , i.e., the difference between T_C and T_g . For this composition, ΔT is 215 °C. So, a large sintering time should be applied in this interval if the objective is to obtain a very dense body⁴. In fact, Figure 4a, which shows the thermogram (DTA) of the glass, exhibits two exothermic crystallization peaks: T_{C1} at 810 °C and T_{C2} at 915 °C. According to Figure 5, these crystallization peaks are related to the formation of the zircon ($ZrSiO_4$, JCPDS 01-083-1374) and β -spodumene ($LiAlSi_2O_6$, JCPDS 00-035-0797) crystalline phases, respectively. Figure 4a shows that the crystallization process starts at about 760 °C and extends up to 920 °C. This interval of crystallization is in good agreement with the interval of "quasi" interruption of sintering (Figure 4b).

Figure 4b shows the sintering behavior, based on thermal shrinkage measurements, of the investigated composition. According to this figure, sintering starts at about 620 °C, achieves a maximum sintering rate at 710 °C, and continues up to 800 °C. At this temperature, the sintering rate almost reached zero, due to the start of crystallization. During the crystallization time, the thermal shrinkage showed no change. After crystallization, the material resumed shrinking around 1020 °C. The mechanism of sintering in that temperature was viscous flow of the remaining glass, since the material was not yet fully crystalline. At 1020 °C, the thermal shrinkage was found

to be 13.9%. After that, the material entered the expansion process before melting completely.

The starting point of the sintering process is related to the glass transition temperature, as discussed previously. Moreover, Figure 6

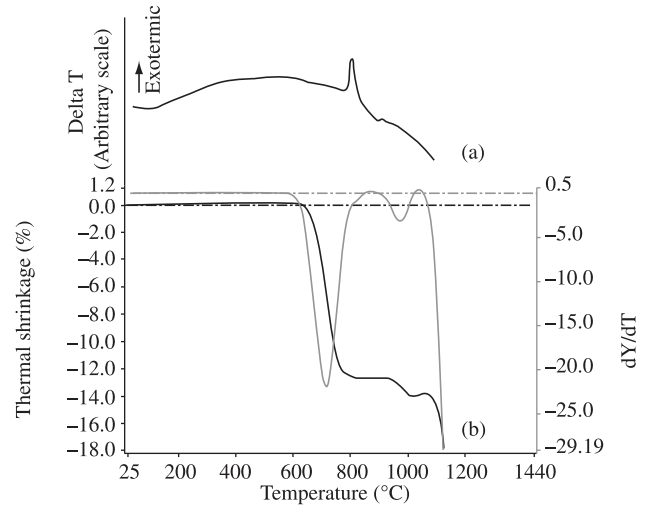


Figure 4. Thermal analysis of the investigated composition: (a) differential thermal analysis and (b) thermal shrinkage.

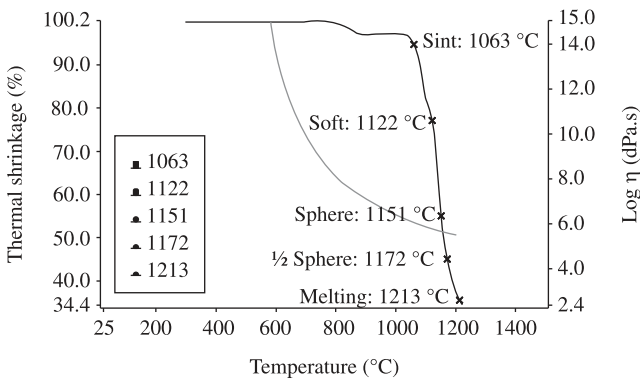


Figure 3. Viscosity behavior of the glass.

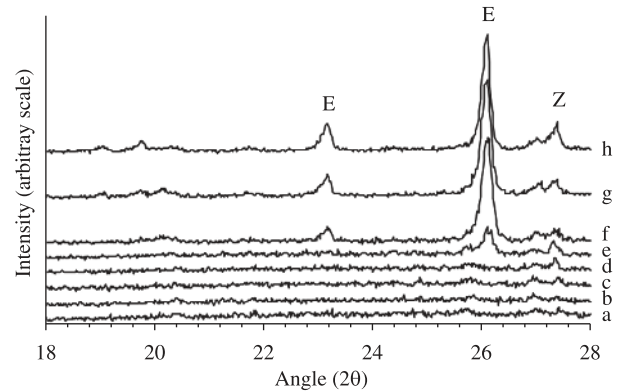


Figure 5. X ray diffraction patterns for the investigated composition heat treated at several temperatures: (a) room temperature; (b) 700 °C; (c) 750 °C; (d) 800 °C; (e) 850 °C; (f) 900 °C; (g) 950 °C; and (h) 1000 °C. E - β -spodumene; Z - zircon.

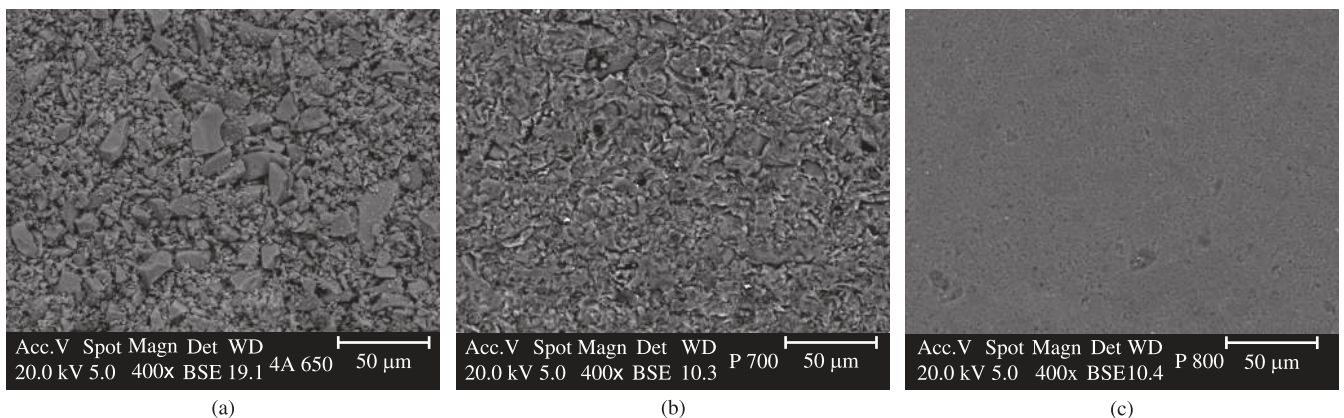


Figure 6. SEM observation of the microstructural evolution of the investigated composition during the sintering process at: (a) 650 °C; (b) 700 °C; and (c) 800 °C.

shows the evolution of the sintering process. At 650 °C, particles are not yet interconnected through the necks, while at 700 °C, the interconnection among particles can be observed in the structure. Finally, at 800 °C, the microstructure presents a denser and more continuous structure.

As shown in Figure 4b, the maximum thermal shrinkage was obtained at 1020 °C. In order to define a suitable time for achieving the maximum densification at that temperature, a sample was heat treated at 1020 °C for a long time. Figure 7 shows the thermal shrinkage as a function of the heat treatment time. After the material was kept for 180 minutes at 1020 °C, the thermal shrinkage changed from 13.9 to 15.4%.

A study is currently being carried out to improve the sintering process and to investigate the crystallization process more deeply.

4. Conclusions

A glass-ceramic composition based on the LZSA system was produced by sintering and crystallization of a parent glass powder (3.68 μm average particle diameter). Sintering started at about 620 °C and was almost completed by 800 °C because of the beginning of the crystallization process. The zircon and β -spodumene crystalline phases crystallized between 810 and 920 °C. After crystallization, the material began shrinking at 1020 °C. When held at this temperature for 180 minutes, the material achieved a thermal shrinkage of 15.4%.

Acknowledgements

The authors are grateful to CNPq/Brazil for funding this work.

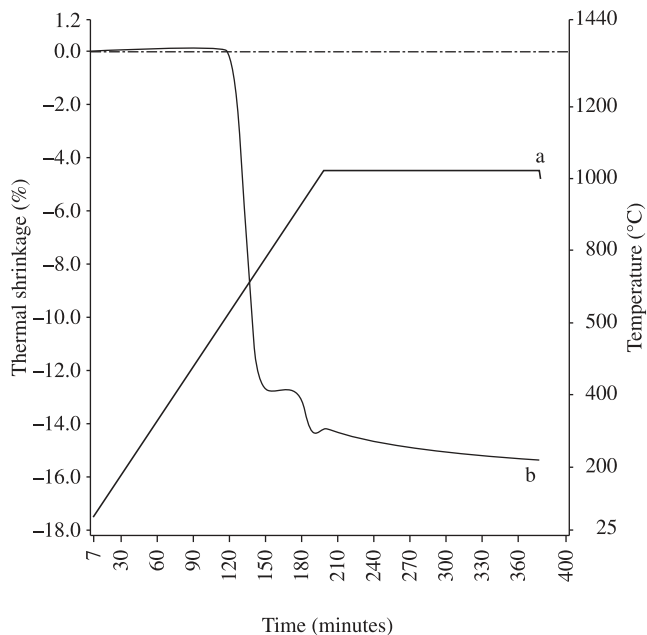


Figure 7. Thermal shrinkage and heating rate as a function of the heat treatment time of the investigated composition heat treated at 1020 °C for 180 minutes: (a) heating rate; (b) thermal shrinkage

References

- Pannhorst W. Overview. In: Bach H (editor). *Low thermal expansion glass ceramics*. Germany: Springer; 1995. p. 1-12.
- Rincon JM, Romero M. Los materiales vitrocerámicos en la construcción. *Materiales de construcción*. 1996; 46(242-243):91-106.
- Novaes de Oliveira AP, Manfredini T, Leonelli C, Pellacani, GC. Physical properties of quenched glasses in the Li₂O-ZrO₂-SiO₂ system. *Journal of the American Ceramic Society*. 1996; 79(4):1092-1094.
- Montedo ORK. *Projeto, caracterização e preparação de camada de proteção para revestimento cerâmico constituída por vitrocerâmico do sistema LZSA* [tese]. Florianópolis: Universidade Federal de Santa Catarina; 2005. 140 p.
- Gomes CM. *Produção e caracterização de laminados vitrocerâmicos do sistema Li₂O-ZrO₂-SiO₂-Al₂O₃ (LZSA) por manufatura de objetos laminados (LOM)* [tese]. Florianópolis: Universidade Federal de Santa Catarina; 2008. 118 p.
- Reitz GM, Montedo ORK, Alarcon OE, Hotza D, Novaes de Oliveira AP. Roll pressed LZSA glass-ceramics. *Advances in Science and Technology*. 2006; 45:442-446.
- Gomes CM, Biscaia FN, Quinaud JT, Montedo ORK, Novaes de Oliveira AP, Hotza D. Aqueous tape casting of LZSA glass ceramics. *Ceramic Transactions*. 2006; 193: 9-16.
- Montedo ORK, Reitz GM, Bertan FM, Novaes de Oliveira APN, Hotza D, Siligardi C. Extruded LZS glass-ceramics. *American Ceramic Society Bulletin*. 2004; 83(8):9201- 9206.
- Giassi L, Montedo ORK, Hotza D, Fredel MC, Novaes de Oliveira AP. Injection moulding of Li₂O-ZrO₂-SiO₂-Al₂O₃ (LZSA) glass-ceramics. *Glass Technology*. 2005; 46(3):277-280.
- Montedo ORK, Bertan FM, Piccoli R, Hotza D, Klein AN, Novaes de Oliveira AP. Low thermal expansion sintered LZSA glass-ceramics. *American Ceramic Society Bulletin*. 2008; 87(7):34-47.
- Reitz GM, Montedo ORK, Comini E, Mundstock KB, Hotza D, Novaes de Oliveira AP. Revestimentos obtidos por laminação de pós de precursor vitrocerâmico do sistema LZSA. *Cerâmica Industrial*. 2008; 13(6):1-5.
- Siligardi C, D'Arrigo MC, Leonelli C. Sintering behavior of glass-ceramic frits. *American Ceramic Society Bulletin*. 2000; 79(9).
- Paganelli M. Studying frits with the heating microscope. *Ceramic World Review*. 1997; 24/97:148-152.
- Paganelli M. Understanding the behaviour of glazes: new tests possibilities using the automatic hot stage microscope "Misura". *Industrial Ceramics*. 1997; 17(2):69-73.
- Paganelli M. Nuove prospettive di studio del comportamento dei vetri e delle fritte ceramiche grazie alla analisi automática delle immagini fornite dal microscopio riscaldante. *Ceramurgia*. 1997; 4:232-238.
- Frenkel J. Viscous flow of crystalline bodies under the action of surface tension. *Journal of Physics (USRR)*. 1945; 9(5):385-391.
- Shyu JJ, Lee HH. Sintering, crystallization, and properties of B₂O₃/P₂O₅ doped of Li₂O·Al₂O₃·4SiO₂ glass-ceramics. *Journal of the American Ceramic Society*. 1995; 78(8):2161-2167.
- Zanotto ED. Isothermal and adiabatic nucleation in glass. *Journal of Non-Crystalline Solids*. 1987; 89(3):361-370.
- James PF, Jones RW. Glass ceramics. In: Cable M, Parker JM. (editors). *High-performance glasses*. New York: Blackie, Glasgow; 1992. p. 102-113.